2005 International Symposium on Nonlinear
Theory and its Applications (NOLTA2005)
Bruges, Belgium, October 18-21, 2005

A Hopf-type generalized van-der-Pol oscillator underlies active signal generation in *Drosophila* hearing

R. Stoop [*], A. Kern [*], M.C. Göpfert [+], D.A. Smirnov [†], T.V. Dikanev [°], B.P. Bezrucko [°]

[*] Institute of Neuroinformatics, University / ETH Zürich, 8057 Zürich
[+] Institute of Zoology, University of Cologne, 50923 Cologne, Germany
[†] Institute of RadioEngineering and Electronics of the Russian Academy of Sciences, Saratov 410019, Russia
[°] Saratov State University, Saratov 410026, Russia
Email: ruedi@ini.phys.ethz.ch, ruedi@ini.phys.ethz.ch

Abstract—The antennal hearing organs of the fruit fly *Drosophila melanogaster* boost their sensitivity by an active mechanical process that, analogous to the cochlear amplifier of vertebrates, resides in the motility of mechanosensory cells. This process nonlinearly improves the sensitivity of hearing and occasionally gives rise to self-sustained oscillations in the absence of sound. Time series analysis of self-sustained oscillations now unveils that the underlying dynamical system is well described by a generalized van-der-Pol oscillator. From the dynamic equations, the underlying active mechanism can explicitly be derived. According to the model, the *Drosophila* hearing organ is driven by a regenerative amplifier that displays a Hopf-type nonlinearity, emphasizing the functional parallels between insect and vertebrate ears.

1. Introduction

The cochlear amplifier is a fundamental, generally accepted concept in cochlear mechanics, having a large impact on our understanding of how hearing works. The concept, first brought forward by Gold in 1948 [1], posits that an active mechanical process improves the mechanical performance of the ear [2]. Until recently, the study of this amplificatory process has been restricted to the ears of vertebrates, where the high complexity and the limited accessibility of the auditory system complicate the in situ investigation of the mechanisms involved. This limitation has hampered the validation of cochlear models that have been devised (e.g., [3, 4]). The hearing organs of certain insects have recently been shown to exhibit signal processing characteristics similar to the mammalian cochlea by using active amplification [5, 6, 7]: the ears of these insects are able to actively amplify incoming stimuli, display a pronounced compressive nonlinearity, exhibit power gain, and are able to generate self-sustained oscillations in the absence of sound. In both vertebrates and insects, the mechanism that promotes this amplification resides in the motility of auditory mechanosensory cells, i.e. vertebrate hair cells and insect chordotonal neurons. Both types of cells are developmentally derived by homologous genes and share similar transduction machineries, pointing to a common evolutionary origin [8]. In line with such an evolutionary scenario, it seems possible that also the fundamental mechanism of active amplification in the ears of insects and vertebrates is evolutionary conserved [9].

Since insect hearing organs are located on the body surface (head, thorax, legs etc.), they are accessible to non-invasive examination. Moreover, because the external sound receiver is often directly coupled to the auditory sense cells, insect auditory systems can be expected to provide profound experimental and theoretical insights into the in situ mechanics of motile sense cells and their impact on the mechanical performance of the ear. Such information is technically relevant: providing natural examples of refined active sensors, the minuscule ears of insects promise inspiration for the design of nano-scale artificial analogues. Hardware solutions mimicking signal-processing characteristics of the mammalian cochlea have already been devised, the responses of which are hardly distinguishable from the biological example [10, 11].

In this contribution, we model self-sustained oscillations of the antennal ear of the fruit fly *Drosophila melanogaster*. By using time-series analysis methods, we reconstruct the generating differential equation and we show that the amplificatory process is well-described by a generalized van-der-Pol equation. The fly's auditory system is shown to be driven by a regenerative amplifier, as was proposed by Gold [1] for the cochlear amplifier of vertebrates.

2. Limit-cycle oscillations

In *Drosophila*, hearing is mediated by mechanosensory neurons that directly connect to an external sound receiver formed by the antenna's distal part [6]. These neurons actively modulate the receivers mechanics and, occasionally, give rise to self-sustained receiver oscillations (SO). SO occur spontaneously and are reliably induced by thoracic injection of dimethyl-sulphoxide (DMSO), a local analgesic known to affect insect auditory transduction. The precise action of DMSO on the auditory neurons remains unclear. However, as spontaneous and DMSO-induced SO are both physiologically vulnerable and display similar temporal patterns, the latter can be used to probe the

nature of the amplificatory mechanism in the fly's antennal ear [5]. As revealed by measurements of the receiver's vibrations, about 20 min after administration of DMSO fully developed SO are observed (Fig. 1b). They have the shape of relaxation oscillations, with a characteristic frequency of about 100 Hz [6]. About 10 min later, the SO start to decrease in amplitude (Fig. 1c) and finally converge towards a sinusoidal form (Fig. 1d). The evoked SO may last up to 1 - 1.5 hours.

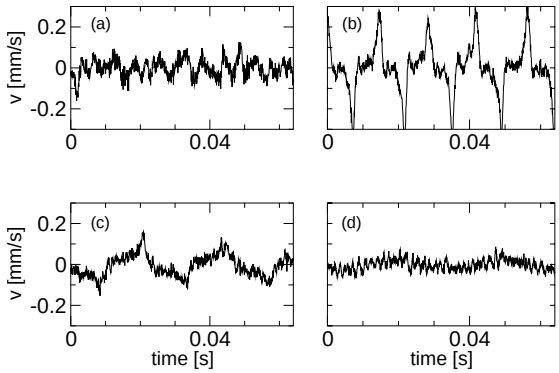

Figure 1: Self-sustained oscillations of the *Drosophila* hearing sensor (velocity measurements), (a) 10 min, (b) 20 min, (c) 30 min, (d) 34 min after DMSO injection.

The shape of these oscillations are reminiscent of limit-cycle oscillations generated by a van-der-Pol type oscillator,

$$\ddot{x} - \mu(1 - x^2)\dot{x} + x = 0, \tag{1}$$

where x is identified with the receiver's vibrational position and where the control parameter $\mu > 0$ is slowly decreased in order to account for the changes of SO shapes during time. It is well known that at $\mu = 0$, the van-der-Pol oscillator undergoes a Hopf bifurcation: For $\mu > 0$, stable limit cycles emerge that can be interpreted as undamping (i.e. amplification). A more detailed examination of the experimental data reveals a pronounced asymmetry (see Fig. 1 (b)) by comparing the onsets and extents of the upward and downward excursions within one period, that requires a more general model for SO generation than the standard van-der-Pol system.

In order to capture this asymmetry, our modeling is based on the generalized van-der-Pol oscillator

$$\ddot{x} + P_n(x)\dot{x} + P_m(x) = 0, \tag{2}$$

where $P_n(x)$ and $P_m(x)$ describe polynomials of order n and m, respectively. From the point of physics, $P_n(x)$ describes a nonlinear, and possibly negative, friction, whereas $P_m(x)$ describes a nonlinear restoring force. Our objective is to determine the orders n, m and the polynomial coefficients that yield the optimal reproduction of the experimental data. We expect that for a proper model, the polynomial orders n and m are unambiguously determined, and only the variation of the coefficients will account for the observed changes in the SO shapes over time.

3. Model construction

From the measurements, we are provided with a time series of the receiver's vibration velocities. In order to determine the optimal model, additional information about the displacement and the acceleration is required. These are determined by numerical integration and differentiation, respectively. For both cases, characteristic difficulties must be overcome. In the case of the receiver position, slow changes in the mean velocity induce a significant drift in the computed locations. This drift can be eliminated by approximating the computed locations by a polynomial in the least-squares sense and subtracting the polynomial values from the location values. Using a polynomial of 20th order, the nonlinear trends are annihilated, including the linear and the quadratic contributions. Unfortunately, high-order polynomials induce strong oscillations in the vicinity of the beginning and end of the time series. For the further analysis, these parts of the time series must therefore be excluded. In the case of the numerical differentiation, in order to reduce the effects of the noise, the measured noisy time series must be smoothed. By applying a first order Savitsky-Golay filter [12], this can be achieved in an efficient way.

As the basis for our generalized van-der-Pol fit to the data, we consider polynomials of the form

$$f(x, \dot{x}) = -P_n(x)\dot{x} - P_m(x). \tag{3}$$

In this notation, the differential equation takes the form

$$\ddot{x} = f(x, \dot{x}). \tag{4}$$

In order to determine the optimal polynomial orders, for each (n, m) order model the polynomial coefficients that minimize the squared error

$$\epsilon^2_{n,m} = \sum_{i=1}^{N} \left(\ddot{x}(t_i) - f(x(t_i), \dot{x}(t_i))\right)^2, \tag{5}$$

are determined, where the time series $\{\ddot{x}(t_i)\}$ were normalized to have unit variance. Since the time series are non-stationary, the time steps t_i at which $\dot{x}(t_i)$ is measured should be restricted to a quasistationary subset of the entire time series. The lengths N of these subsets ($\sim$ 4000 data points) were found to be large enough in order that polynomial fitting can be reliably performed.

It is observed that the error $\epsilon^2_{n,m}$ saturates for $n = 2$ and $m = 5$ (Fig. 2). A further increase of $\{n, m\}$ does not reduce

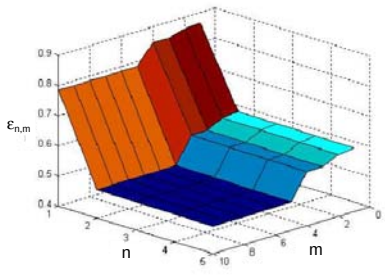

Figure 2: Root-mean-squared error $\epsilon_{n,m}$ of the model fitting Eq. (5), showing a precipitous decay and saturation of the error around the orders $n = 2$ and $m = 5$ of the polynomial approximation.

$\epsilon^2_{n,m}$. The emergence of such a conspicuous saturation point is a very rare case and indicates that the model structure (2) faithfully reproduces the auditory data of *Drosophila*. It could be argued that the relatively high noise level prevents the error $\epsilon^2_{n,m}$ from decreasing any further. In the absence of noise, the errors might thus gradually decrease with increasing $\{n, m\}$. Fortunately, the rapid decay of $\epsilon_{n,m}$ before saturation is a strong evidence against this view, indicating that our modeling is realistic indeed. Moreover, noise-cleaned [13] experimental data reveal a basically unchanged decay behavior, which corroborates the validity of the obtained optimal polynomial orders.

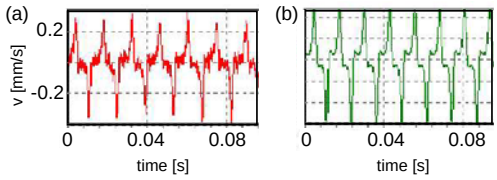

Figure 3: (a) Receiver's vibration velocity observed 20 min after DMSO injection (fully developed SO). (b) Approximating time series generated by the model (2), using $n = 2$ and $m = 5$.

A comparison between realizations of time series by the model and the measurements corroborates the validity of our modeling. For the fully developed SO (after 20 minutes, see Fig. 4), the comparison reveals that the measured velocities are faithfully reproduced. This is further illustrated in Fig. **??**, where the modelled and the measured data are compared in the phase plane $(x, \dot{x})$, where the positions x were obtained by numerical integration from the measured velocities. Similar observations emerge for the time series recorded 10, 30, and 34 minutes, respectively, after DMSO injection.

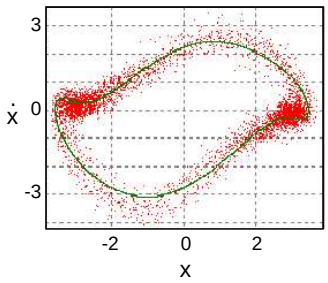

Figure 4: Phase-space representation of measured (dots) and modelled (solid line) receiver vibrations (at fully developed SO).

4. Amplification dynamics

The shapes of the polynomials $P_n(x)$ and $P_m(x)$ reflect the asymmetry of the observed receiver oscillations, specifically when the SO are fully developed (cf. Fig. 1 (b)). The asymmetry of $P_n(x)$ and, in particular, $P_m(x)$ (see Fig. 5 (b)) becomes effective at large displacements and may have its origin in structural-mechanical properties of the antenna. An enlightening interpretation of the amplification dynamics can be given for the behavior around zero displacement position $x \cong 0$, where $P_n(x)$ attains negative values for small displacements x (Fig. 5 (a)). Since $P_n(x)$ represents a nonlinear friction, $P_n(x) < 0$ implies that energy is injected into the system. This is a characteristic feature of an active amplification processes. Around $x = 0$, the nonlinear restoring force $P_m(x)$, together with its first and second derivatives, are relatively small. This implies that for small receiver displacements, virtually no restoring force is present. By means of the negative friction term, the system is thus easily driven out to relatively large amplitudes.

In the course of time, i.e. with decreasing DMSO concentration, the nonlinear contributions to friction and restoring force decay. In particular, the range where the friction is negative, gradually decreases and finally vanishes, in agreement with the observed reduction in SO amplitude (see Fig. 1). When the SO start to disappear, the restoring force function $P_m(x)$ obtains an approximately linear characteristic with a very small slope. At the same time, the friction term remains to be very small. As a consequence, weak stimuli will be sufficient to elicit considerable antennal vibrations. Although the amplifier has now returned into a stable state, where limit-cycles do not occur, it remains very sensitive. Only small parameter variations are necessary in order to render the friction term negative and to lead to an amplification of incoming vibrations.

Our results may be compared to measurements of active hair-bundle oscillations of vertebrate hair cells, pointing to a slight difference in the mechanisms involved. Active hair bundle oscillations promote active amplification in non-mammal and, possibly, mammal vertebrates [14, 15, 16].

Mechanical stimulation experiments performed on isolated hair bundles have shown that the bundle stiffness may become negative for small bundle displacements [16, 15]. In this case, bundle stiffness has its origin in the amplification-promoting ion-channel dynamics. For the *Drosophila* hearing sensor, our model suggests that amplification emerges from negative friction; only at intermediate displacements, regions of negative stiffness are found (Fig. 5b).

Recently, it was proposed that active amplification in the mammalian hearing system is governed by the generic Hopf-type differential equation [17]. It was later demonstrated that a Hopf-type cochlea model is indeed able to faithfully reproduce measured cochlea responses [4]. Moreover, based on this model, the cochlear processing of multi-frequency tones is easily explained [18]. Due to the dominating nature of the Hopf nonlinearity, this model is compatible with the present van-der-Pol system Eq. (1), known to also exhibit a Hopf bifurcation at $\mu = 0$. Active amplification using Hopf nonlinearities thus appears to be a general mechanism in biological sensing. Finally, a comparison with approaches of modeling spontaneous otoacoustic emissions (SOAE) by means of active nonlinear oscillators can be made. It was recently shown [19] that in order to generate the correct exponential relaxation part behavior of SOAE, the simplest van der Pol oscillator variant (1) is insufficient. To correct this, the damping coefficient term $(1 - x^2)$ was changed into the form $(\frac{c}{(\langle x^2 \rangle)^m} - b)$, where c, b, m are positive numbers and $\langle \cdot \rangle$ denotes the average over many cycles of the inherent oscillations of the system. The fractional term has the effect that the nonlinear active amplification term (undamping) grows significantly in the neighborhood of $x = 0$, whereas linear damping dominates for larger amplitudes. This yields the experimentally observed exponential relaxation behavior at intermediate relaxation time. For the implementation of the also observed initial saturation regime, an additional (negative quadratic) term is required. Fig. 5 and a numerical check shows that these experimental features are already built into our model.

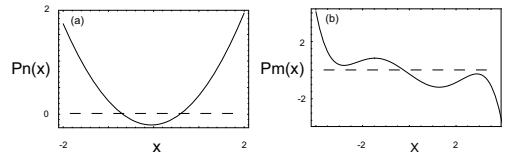

Figure 5: (a) Nonlinear friction $P_n(x)$, showing undamping ($P_n(x) < 0$, dashed line), (b) nonlinear restoring force $P_m(x)$, displaying a noticeable asymmetry. Fully developed SO 20 min after DMSO injection, approximated by polynomials of degrees $n = 2$ and $m = 5$.

References

[1] T. Gold, "The physical basis of the action of the cochlea", *Proc. R. Soc. Lond. B*, vol. 135, pp. 492–498 (1948).

[2] L. Robles, M.A. Ruggero, "Mechanics of the mammalian cochlea", *Physiol. Rev.*, vol. 81, pp. 1305–1352 (2001).

[3] P. Dallos, A.N. Popper, R.R. Fay (eds.), "The Cochlea. Springer Handbook of Auditory Research", Springer (1996).

[4] A. Kern, R. Stoop, "Essential role of couplings between hearing nonlinearities", *Phys. Rev. Lett.*, vol. 91, pp. 128101 1–4 (2003).

[5] M.C. Göpfert, D. Robert, "Active auditory mechanics in mosquitoes", *Proc. R. Soc. Lond. B*, vol. 268, pp. 333–339 (2001).

[6] M.C. Göpfert, D. Robert, "Motion generation by *Drosophila* mechanosensory neurons", *Proc. Natl. Acad. Sci. USA*, vol. 100, pp. 5514–5519 (2003).

[7] M.C. Göpfert, A.D.L. Humpfries, J.T. Albert, D. Robert, O. Hendrich, "Power gain exhibited by motile neurons in *Drosophila* ears", *Proc. Natl. Acad. Sci. USA*, vol. 102, pp. 325–330 (2005).

[8] G. Boekhoff-Falk, "Hearing in *Drosophila*: development of Johnston's organ and emerging parallels to vertebrate ear development", *Dev. Dyn.*, vol. 232, pp. 550–558 (2005).

[9] D. Robert, M.C. Göpfert, "Novel schemes for hearing and orientation in insects", *Curr. Opin. Neurobiol.*, vol. 12, 715–720 (2002).

[10] J.-J. van der Vyver, A. Kern, R. Stoop, "An electronic Hopf cochlea", patent submitted (2005).

[11] R. Sarpeshkar, R.F. Lyon, C.A. Mead, "A low-power wide-dynamic-range analog VLSI cochlea", *Analog Integrated Circuits and Signal Processing*, vol. 16, pp. 245–274 (1998).

[12] A. Savitsky, M.J.E. Golay, "Smoothing and differentiation of data by simplified least square procedures", *Anal. Chem.*, vol. 36, pp. 1627–1639 (1964).

[13] A. Kern, W.-H. Steeb, R. Stoop, "Projective noise cleaning with dynamic neighborhood selection", *Int. J. Mod. Phys. C*, vol. 11, pp. 125–146 (2000).

[14] D.K. Chan, A.J. Hudspeth, "Ca2+ current-driven nonlinear amplification by the mammalian cochlea in vitro", *Nat. Neurosci.*, vol. 8, pp. 149-155 (2005).

[15] H.J. Kennedy, A.C. Crawford, R. Fettiplace, "Force generation by mammalian hair bundles supports a role in cochlear amplification", *Nature*, vol. 433, pp. 880–883 (2005).

[16] P. Martin, A.D. Mehta, A.J. Hudspeth, "Negative hair-bundle stiffness betrays a mechanism for mechanical amplification by the hair cell", *Proc. Natl. Acad. Sci. U.S.A.*, vol. 97, pp. 12026–12031 (2000).

[17] V.M. Eguíluz, M. Ospeck, Y. Choe, A.J. Hudspeth, M.O. Magnasco, "Essential nonlinearities in hearing", *Phys. Rev. Lett.*, vol. 84, pp. 5232–5235 (2000).

[18] R. Stoop, A. Kern, "Two-tone suppression and combination tone generation as computations performed by the Hopf cochlea", *Phys. Rev. Lett.*, vol. 93, pp. 268103 1–4 (2004).

[19] R. Sisto, A. Moleti, "Modeling otoacoustic emissions by active nonlinear oscillators", *J. Acoust. Soc. Am.*, vol. 106, pp. 1893–1906 (1999).